Design and Co-Analysis of a Permanent Magnet Brushless DC Motor by Using Clonal Selection Principle Based Wound Healing Algorithm and Ansys-Maxwell

Yıldırım ÖZÜPAK[1*]   Mehmet ÇINAR[2]

[1] Silvan Vocational School, Dicle University, Diyarbakır, Türkiye
[2] Tatvan Vocational School, Bitlis Eren University, Bitlis, Türkiye

Keywords	Abstract
BLDC WHA Optimization PID Controller	This paper presents the design and analysis of a 550 W Permanent Magnet (PM) Brushless DC motor (BLDC). The finite element method (FEM) was employed to assess the motor's performance characteristics. The design and dynamic performance analysis were conducted using ANSYS/Rmxprt, while electromagnetic studies were carried out using ANSYS/Maxwell-2D. Additionally, optimization of the DC motor was achieved through a Wound Healing Algorithm (WHA). A PID controller was designed for this purpose. The paper also elaborates on the detailed design equations for creating a BLDC motor. BLDC motors are known for their high dynamic responses, efficiency, extended operating life, wide speed change intervals, and noise-free operation. The motor's geometry was modeled in the ANSYS-Maxwell-Rmxprt software tool and later imported into the Maxwell-2D environment for further analysis. The designed motor was observed to operate with 93% efficiency, meeting the specified torque value. The results of the optimization process were interpreted by comparing them with the values obtained from the ANSYS software.

1. INTRODUCTION

In recent years, Brushless Direct Current (BLDC) motors have garnered significant attention in the industry due to their substantial advantages. The pre-diagnosis of malfunctions is a crucial aspect in these motors since any malfunction can impact the motor's sensitivity. Recent developments in permanent magnets have facilitated their use in electrical machines. The replacement of conventional field windings in the rotor of traditional DC motors with permanent magnets enhances efficiency by reducing copper losses. These permanent magnet motors find widespread use in various industrial applications owing to their high torque, flexible design, and excellent efficiency and dynamic performance characteristics.

Studies on permanent magnet motors started in the 1990s. The detailed study of the magnetic equivalent circuit design of these motors has started to be carried out by researchers in recent years. Back electromotive force (back emf), harmonic amplitude and winding types between phases and lines have been shaped for different groove structures and magnet numbers. ANSYS-Maxwell-3D was used to design motors with different grooves and pole numbers and detailed analysis results were compared with each other (Dusane, 2016). The performance of the motors could be largely predicted even before production.

Multiple design iterations can be conducted faster and at a lower cost, creating new designs by optimizing the original parameters (Özüpak & Aslan, 2023). Precise calculation of motor parameters and features is crucial

---

*Corresponding Author, e-mail: yildirimozupak@gmail.com

for error-free product production (Kannojia & Chinmaya, 2023). This research details the methodology for developing a Brushless DC (BLDC) motor, presenting comprehensive design equations. The motor's geometry is generated through the RMxprt tool in ANSYS. The efficiency of the designed BLDC motor reaches 87.2%, a crucial consideration from an electric vehicle perspective (Kumar et al., 2022). The paper introduces a radial flux Brushless DC (BLDC) motor featuring a distinctive permanent magnet arrangement known as the Halbach-array magnet arrangement. In this arrangement, Halbach-array magnets are strategically positioned between the rotor poles, and their magnetization is configured to enhance the overall air gap flux density. The study conducts a performance comparison with a conventional BLDC motor, utilizing Finite Element Analysis (FEA) solutions to assess the designed configurations (Bala et al., 2020).

Furthermore, the research delves into the performance of a closed-loop BLDC motor with varied slot designs. A two-phase-based control strategy, incorporating a Proportional-Integral (PI) speed controller, is implemented on four types of BLDC motors. These motors are designed with constant slot areas using Ansys software. The study comprehensively analyzes various parameters within the closed-loop system, including dynamic speed response, electromagnetic torque, and air-gap flux waveforms (Kumar et al., 2020). In a study, a firefly algorithm based Fractional-Ordered Proportional-Integral-Derivative (FOPID) controller is proposed for torque and speed control of a Brushless DC (BLDC) motor. The research shows an effective control with low error margin, especially in Matlab/Simulink environment (Ibrahim et al., 2014). In another study, an innovative method for the optimal design of a permanent magnet BLDC motor was introduced (Bapayya & Venkata, 2020). This involves the optimization of electrical and mechanical parameters using a genetic algorithm. In another research, the use of particle swarm optimization (PSO) and bacterial search (BF) algorithms to determine the optimum parameters in a Proportional-Integral-Derivative (PID) controller for BLDC motor speed control was investigated. The study suggests a Fractional-Order PID (FOPID) controller, incorporating the artificial bee colony algorithm to enhance BLDC motor performance. Additionally, the Kalman filter is employed for speed estimation and adjustment. The obtained results are compared with other optimization algorithms, including firefly and particle swarm optimization algorithms. Moreover, a Fractional-Order PID (FOPID) is designed for DC motor speed control in a separate study, utilizing the pollination optimization algorithm. The FOPID parameters are adjusted to obtain optimum operating values, and the results are compared with those obtained from firefly and particle swarm optimization algorithms.

In this study, the design and detailed analysis of the internal magnet BLDC motor operating with a nominal speed of 1504 rpm and operating with 93% efficiency were carried out with two different methods. Transient analysis platform with ANSYS Maxwell 2D was used to obtain the performance values of the motor. The control circuit of the designed motor was designed with Ansys-Scade-Simplorer. With this program, the parameters of the motor, efficiency, speed control, torque, magnetic flux distribution, test results of the motor at full load and at no load were obtained. In addition, the parameters of the motor obtained in the ANSYS program were tried to be obtained with the PID controller designed with the help of the wound healing algorithm and the values were compared with each other.

After the introduction section of this study, the section related to materials and methods has been explained. In the third section of the study, the motor has been analyzed in the ANSYS-Maxwell environment and optimized using the developed algorithm. The fourth section presents the findings of the study as the results.

2. MATERIAL AND METHOD

2.1. Developed Algorithm (wound healing algorithm)

When a foreign substance enters the body, the immune system initiates a response, and the algorithm that leverages the characteristics of this immune response is known as the clonal selection algorithm. The clonal selection principle-based wound healing algorithm is a recently developed algorithm, and its outcomes have been compared with those of a widely used program, such as ANSYS.

$$N_c = \sum_{i=1}^{n} round\left(\frac{N}{i}\right) \tag{1}$$

N_c: Clone numbers that produced from each antigen

N: Solution population's total number

n: Selected antibodies number

The clonal choice principle forms the premise of the wound healing algorithm. With the assistance of equation one, the quantity of clones made is calculated. Wound healing formula was developed with the assistance α (cloning) and f (cloning acceleration factor) parameters other to (1). The ultimate state obtained is given in (4). With the assistance of the new parameters other, a lot of optimized results were tried to be obtained. Developed wound healing algorithm's flow chart is shown in Figure 1. When the initial population P is made, the choice method moves in and selects the antibodies with the most effective immunologic response (affinity) worth to get the new Pn population the essential rule. Throughout the choice process, is that the affinity worth of antibodies. Then, people within the population area unit cloned and new populations area unit created. The quantity of clones to be obtained varies in step with the affinity worth. At this stage, a brand-new population is made by applying hypermutation to the clones. within the hypermutation method, reciprocally proportional to the affinity worth, that is, a low mutation with a high affinity worth encompasses a high mutation rate with a low affinity worth. Thus, antibodies aloof from the optimum resolution area unit subjected to more mutation processes. Then, among the obtained clones, those with low similarity magnitude relation area unit replaced with new ones. As a result, the optimum results obtained with the assistance of biological research and mutation processes.

2.1.1 Solution stages of wound healing algorithm

Utilize N antibodies to form the initial population (P). Evaluate the affinity of each antibody in the P population. Choose the n antibodies (N) with the highest affinity to create a Pn population. To assess the affinity value between an antibody and an antigen, the distance between them is typically considered. This is computed using equation (2) and the Euclidean distance formula.

$$d = \sum_{i=1}^{N}(Ag_i - Ab_i)^2 \tag{2}$$

The computed value of d is compared to the threshold value λ, and the marking error E is determined according to equation (3):

$$E = d - \lambda \tag{3}$$

1. Clone the n antibodies selected in step 2 and construct N_c using (4)

$$Nc_i = \sum_{i=1}^{n} round\left(\frac{a*N_s*f}{i}\right) \tag{4}$$

   α : Cloning factor (value range is 0-1)

Alter the Nc clone population by introducing mutations. Define this subpopulation and calculate the affinity value for each antibody within it. Choose the antibody with the highest affinity value and incorporate it into the original population. Afterwards, replace the low-affinity antibody with new antibodies. In cases where the population value P is less than N, generate antibodies to fill the population.

2.2. Optimum PID Controller Design

There are different controller structures used in control systems. The most used ones are PID, PI, PD, phase advance or phase regression controllers. The PID controller preferred in the study has a wide range of uses due to its many advantages. The number of parameters to be calculated is low, the structure is simple, durable, and reliable, which makes these controllers stand out. PID controllers are controllers that gather the superior aspects of proportional-integral-derivative components under a single structure. While the integral component brings the steady state error closer to zero in the system, the derivative effect increases the response speed of the system. Table 1 displays the parameters WHA. The steady state structure of the PID controller is as follows:

$$U_s = \left(K_p + \frac{K_i}{s} + K_d d\right) E(s) \tag{5}$$

In (6), Kp: Proportional gain, Ki: Integral gain, Kd: Derivative gain.
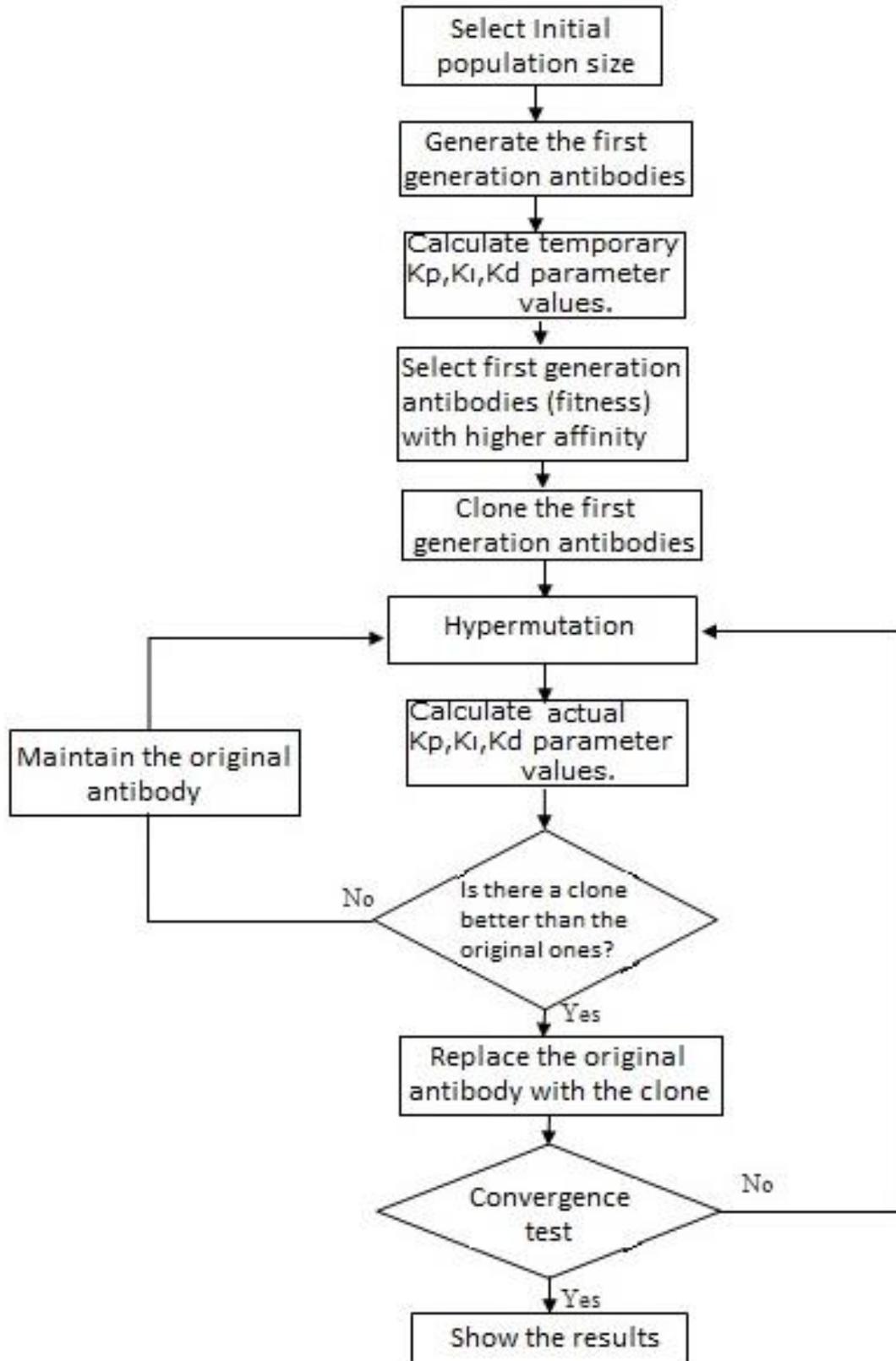
***Figure 1.*** *Wound healing algorithm flowchart*

Table 1. *WHA parameters*

Parameter	Value
Number of Population	150
Iteration number	150
Run number	30
Healing coefficient	1.3
Affinity coefficient	1.3
Clone coefficient (α)	0.4
Clone acceleration (f)	0.95

A Matlab program was created to determine the design values of the permanent magnet brushless DC motor using a developed algorithm. Figure 2 illustrates the screen output of the program, showcasing the calculated PID controller parameter values for the optimization process.
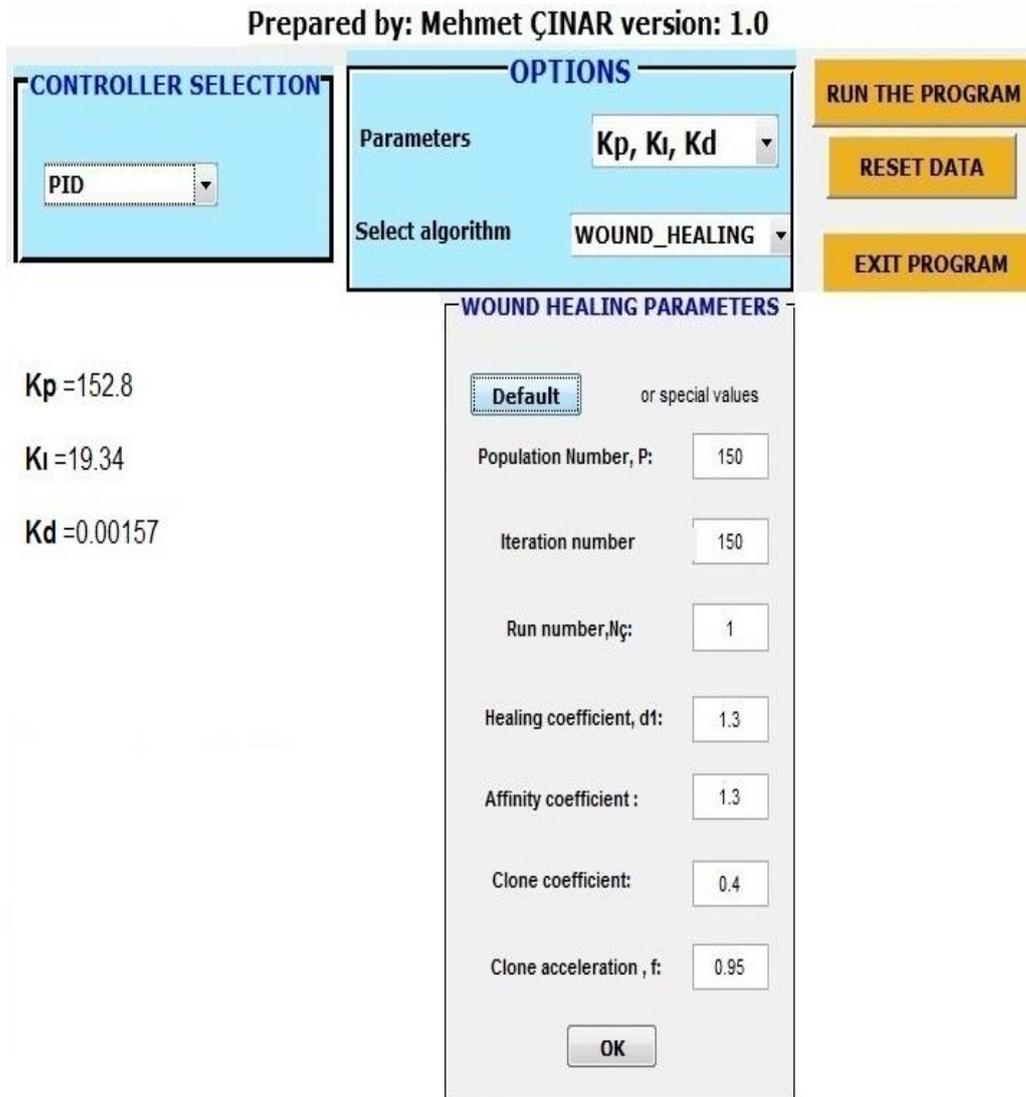
Figure 2. *The Developed Program*

2.3. Mathematical Equations of BLDC

Torque of BLDC motor is expressed by (7).

$$T = 2NN_mB_gLR_{ro}I = k_tI \tag{7}$$

In the given context, where N represents the number of turns in the groove, N_m is the number of poles, Bg is the air gap flux density, L is the length of the motor, and R_ro is the rotor outer diameter. The factor 2N takes into consideration the operation of the three-phase inverter in the 120-degree transmission mode, indicating that 2 phases carry current at any given time. Equation (8) presents the expression for the reverse electromotive force (EMF) in the Brushless DC (BLDC) motor (Bala et al., 2020).

$$E_b = 2NN_mB_gLR_{ro}W_m = k_eI \tag{8}$$

Where W_m is the angular velocity of the rotor. When the torque and reverse EMF equations are compared, it is seen that the torque and back emf constants are equal in (9).

$$k_t = k_e = 2NN_mB_gLR_{ro} \tag{9}$$

Results from the motor can be expressed in terms of main dimensions, specific electric and magnetic charges, and speed. The kVA value of the BLDC motor is given in (10).

$$S = C_oR_{ro}^2LW_m \tag{10}$$

Where, C_o is a constant and is expressed as given in (11).

$$C_o = 11B_{av}ack_w * 10^{-3} \tag{11}$$

Where, B_{av} is the magnetic charge, ac is the electrical charge and k_w is the winding factor.

Copper losses for two phases are given in P_{cu} (12).

$$P_{cu} = 2I^2 \frac{\rho LN^2N_c}{K_{wb}A_g} \tag{12}$$

is expressed as. Here, ρ is the density of the copper wire, N_c is turns, K_{wb} is the filling factor of the bare wire, and A_g is the air gap. Wind and friction losses Pf are given in (13).

$$P_f = \frac{3}{100}P_{out} \tag{13}$$

The weight of the gears of the stator is defined as in equation (14). In the equation, ρ_i represents the iron density, A_t represents the cross-sectional area of the teeth, and N_s the number of grooves.

$$W_t = \rho_iA_tN_sL \tag{14}$$

The weight of the stator yoke is given by (15).

$$W_{sy} = \rho_iA_{sy}L \tag{15}$$

The weight of the rotor yoke is given as in (16).

$$W_{ry} = \rho_iA_{ry}L \tag{16}$$

Total iron weight is calculated as in (17).

$$W_{total} = W_{ry} + W_{sy} + W_t \tag{17}$$

Total iron loss is calculated by (18).

$$P_{iron} = L_{kg} * W_{total} \tag{18}$$

Here L_{kg} is the loss in Watts per kg of stator material. The power input to the motor is calculated with the help of (19).

$$P_{in} = P_{out} + P_{cu} + P_{iron} + P_f \tag{19}$$

Machine efficiency ŋ (%) is given in (20).

$$ŋ \ (\%) = \frac{P_{out}}{P_{in}} \tag{20}$$

2.4. Motor Design

The design motor was made in the Rmxprt part of and Maxwell 2D, which performs the solution with the FEM. The excitation circuit and control circuit of the motor given in Figure 3 were also created in the ANSYS environment. The parameters given in Table 2 and Table 3 are defined as the input parameters of the motor to the software. Figure 3 presents the motor control circuit.

The PID parameter values in the control circuit obtained by the ANSYS program are Kp=150, Ki=20 and Kd=0.0016. These libraries in the program environment allow the parameters and design values to be evaluated at the first stage of the design while the engine is being designed. In this subprogram, analytical parameters can be calculated easily and quickly. The designed engine model can be easily transferred to the Maxwell program in 2D/3D for numerical and electromagnetic analysis. The parameters in Table 2 and their values were used for this design.

Table 2. Stator parameters

Parameter	Value
Ratedpower(W)	550
Ratedvoltage(V)	220
Ratedspeed(rpm)	1500
Number of pole	4
Frictionalloss(W)	12
Windageloss(W)	0

The dimensions of the Slot parameters are presented in Table 3.

Table 3. Slot parameters

Parameter	Value (mm)
Hs0	0.5
Hs1	1
Hs2	8.2
Bs0	2.5
Bs1	5.6
Bs2	7.6

For the rotor permanent magnet pole, the rotor geometry among the shapes in the Rmxprt was used and the parameter values in Table 4 were used for the rotor design.
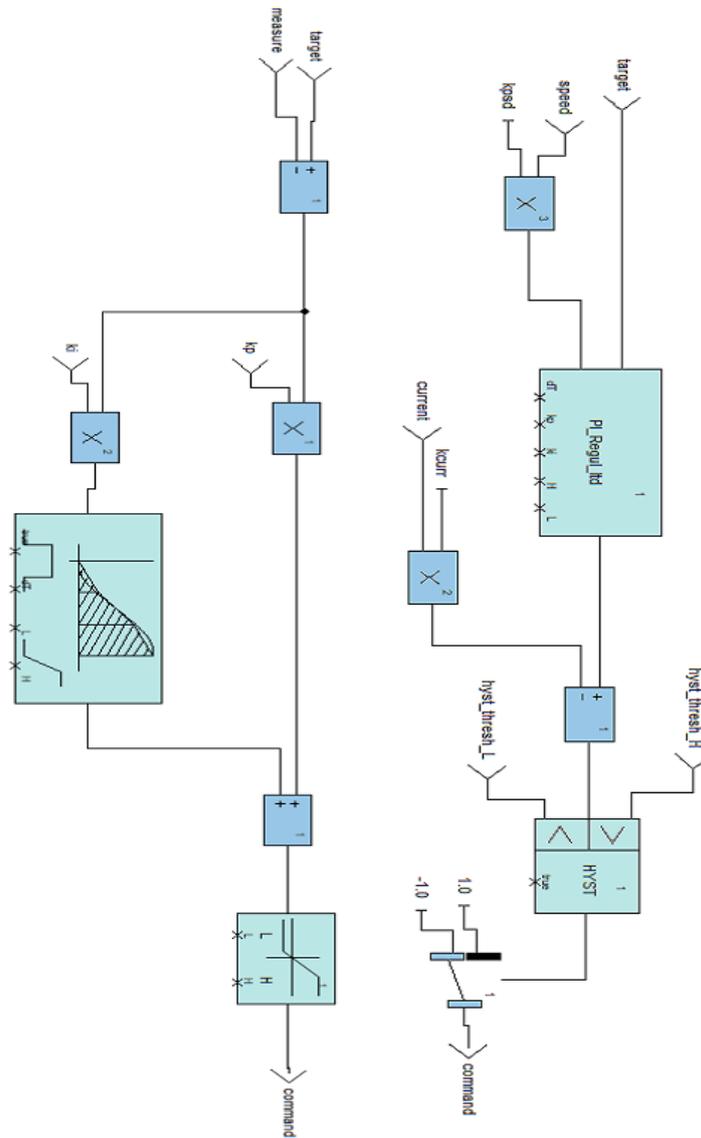
Figure 3. *Motor control circuit*

Table 4. *Rotor parameters*

Parameter	Value
Number of Slots	24
Outer Diameter (mm)	120
Inner Diameter (mm)	75
StackingFactor	0.95
SlotType	2
SkewWidth (mm)	0
Minimum airgap (mm)	1
Type of material	M19_24G
Embrace	0.7
Thickness of magnet (mm)	3.5
MagnetType	XG196/196

3. RESULTS AND DISCUSSION

3.1. Rmxprt Analysis Results

The engine design created in Rmxprt was transferred to the Maxwell-2D environment. This software is used for networking in FEM. There are some analyzes based on simulation in Maxwell 2D. The motor design created in Rmxprt was transferred to the Maxwell-2D environment. This software is used for mesh generation in FEM. Some simulation-based FEM analysis results in Maxwell 2D are presented in Figure 4, Figure 5 and Figure 6. These figures show the mesh formation, magnetic flux distribution, flux lines, speed-efficiency, current-load distribution and magnetic field intensity at a certain time of the rotor position, respectively.
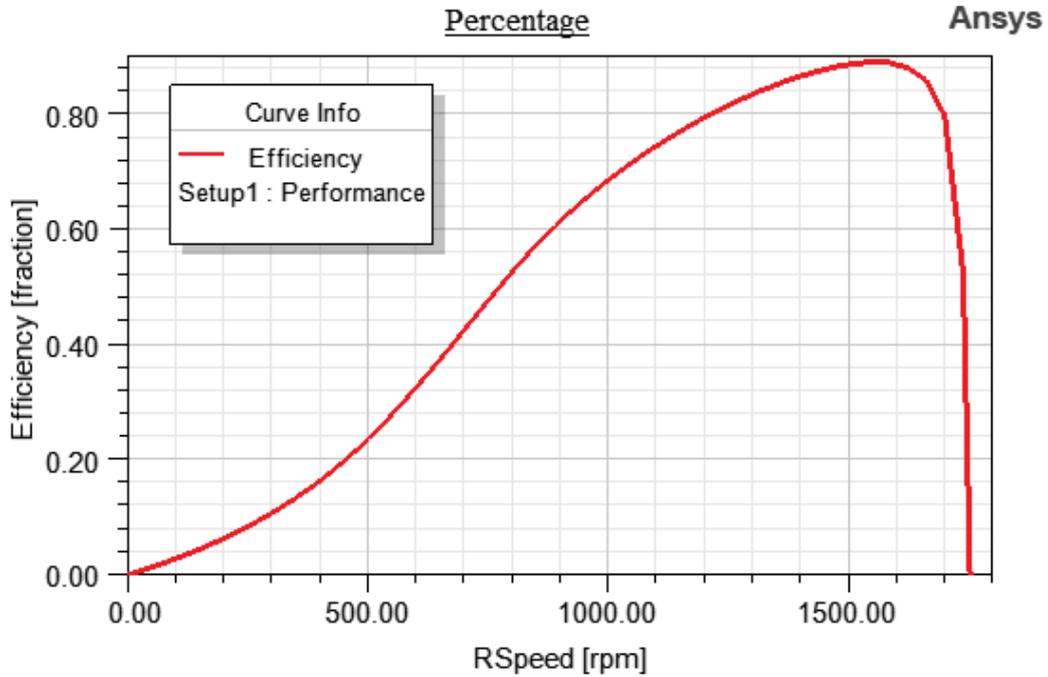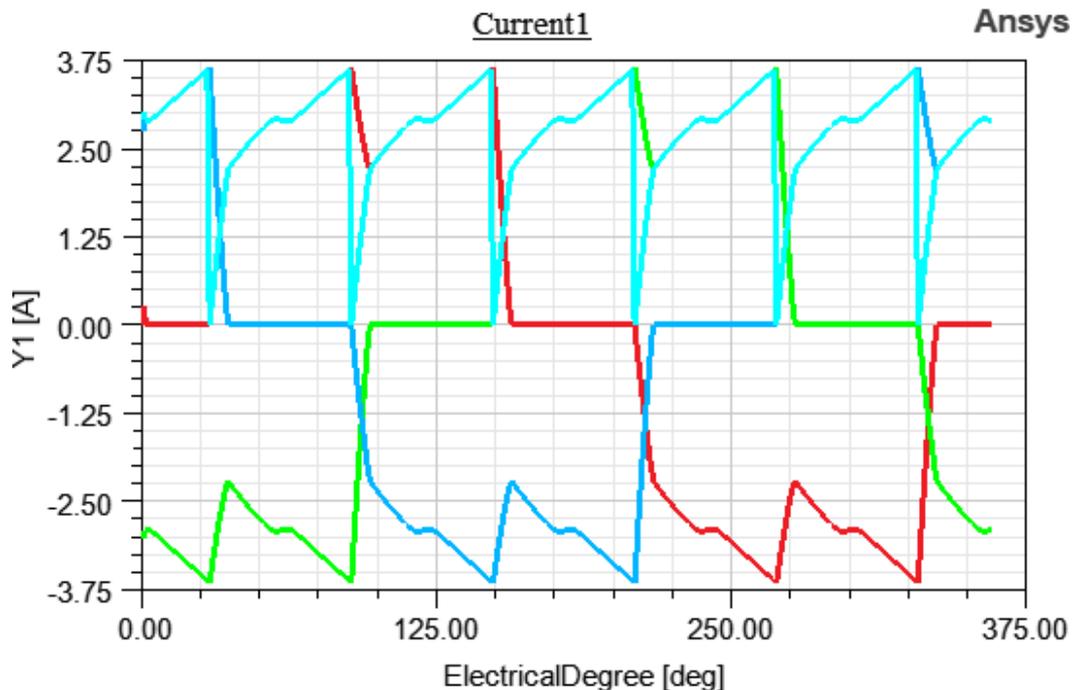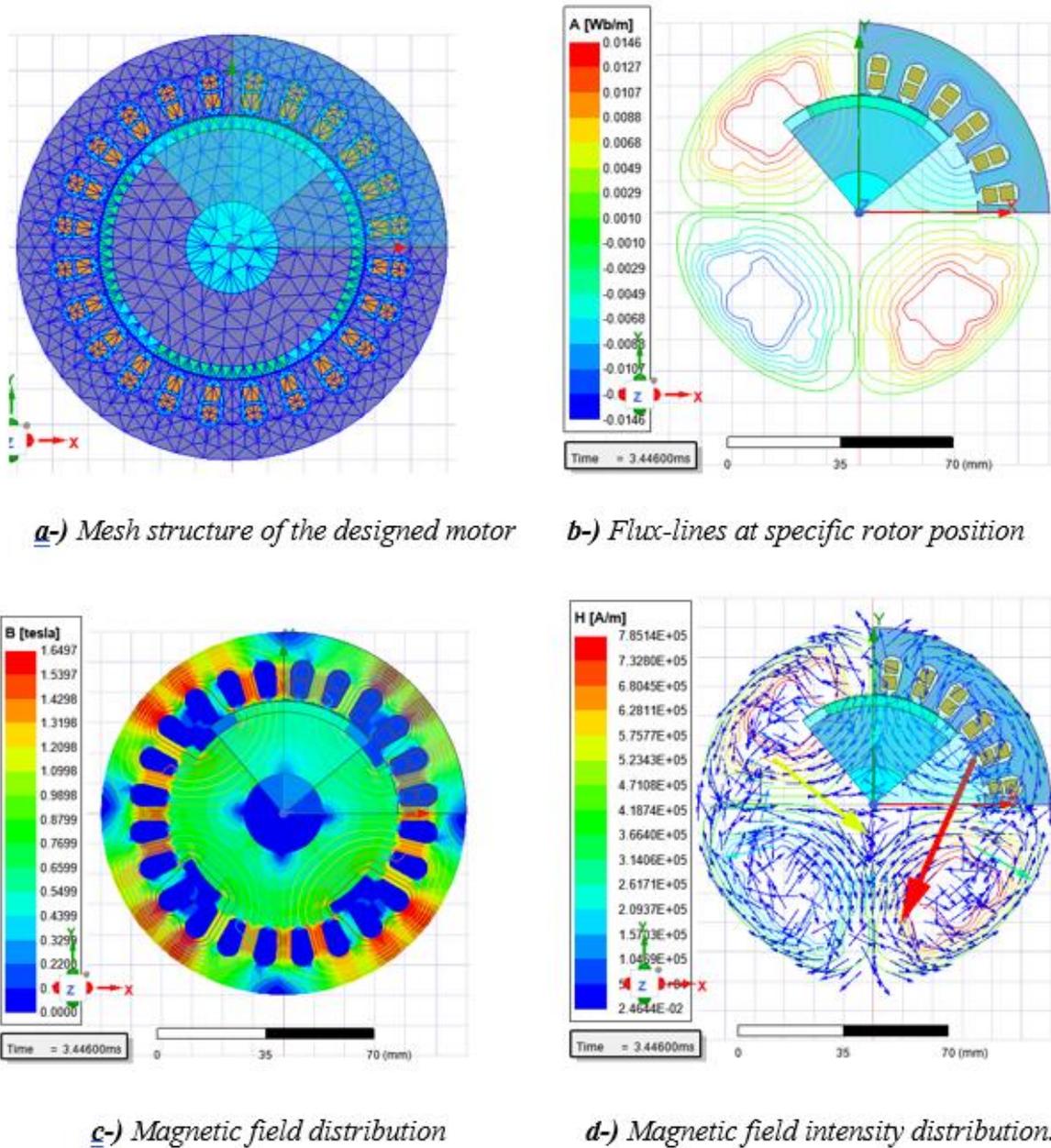

Figure 4. Speed-efficiency graph of the motor

Figure 5. Winding currents of the motor under load and variation of electrical angle graph

a-) Mesh structure of the designed motor   *b-) Flux-lines at specific rotor position*

c-) Magnetic field distribution   *d-) Magnetic field intensity distribution.*

Figure 6. *Electromagnetic Simulations results **a)** Mesh structure of the designed motor; **b)** Flux-lines at specific rotor position; **c)** Magnetic field distribution; **d)** Magnetic field intensity distribution*

After increasing the pole angle of the control circuit on the motor, the analysis is done, and the design is made when the pole angle is 0 degrees. To improve motor performance, the advance angle changes and the change in engine performance is analyzed. After changing the pole angle of the motor, the efficiency of the motor increases. The pole angle determines the induction time of the voltage. The excitation of the previous windings is due to the increase of this pole angle. The phase currents and the opposite electromotive forces of the phases have the same phase angle. Therefore, the desired torque value is obtained from BLDC machines even at low current levels.

3.2. MATLAB Analysis Results

In order to confirm the accuracy of the results obtained, the engine was reanalyzed with the program developed in the MATLAB environment. The values obtained as a result of the ANSYS program, and the results of the developed algorithm are given in Table 5. When Table 5 is examined, it is seen that the obtained values are very close to each other.

Table 5. Results obtained as a result of the analysis

Parameter	Value (ANSYS)	Value (Developed algorithm)
Flux Density (Tesla)	1.34	1.3125
Coercive Force(A/m)	785000	802000
Total Loss(W)	132	130.1
OutputPower(W)	512	508
InputPower(W)	550	550
Efficiency	%93	%92.3
Rated Speed (rpm)	1500	1500
RatedTorque(N-m)	4.01	4.16

4. CONCLUSION

In this paper, the basic design and analysis of the BLDC motor is carried out. Fundamentals of magnetic circuit and necessary basic equations used in electromagnetic field are obtained. BLDC motor with 550 W power and 1500 rpm has been designed. In the study, it has been observed that the efficiency of the motor at nominal torque and nominal speed is very good. The efficiency of the engine was obtained as 93%. The motor was designed in Rmxprt and electromagnetic field analyzes were performed in Maxwell-2D environment. After the motor was designed, the polar angle of the control circuit was changed and analyzes were carried out for different angle values. It has been observed that the efficiency of the BLDC motor increases when this angle is increased from 0° to 30°. It is concluded that by increasing the pole angle, the rated speed of the motor can be increased, an increase in efficiency can be achieved despite a decrease or fluctuation in the rated torque. When the motor parameters obtained in Table 5 with the help of the PID controller were examined, the efficiency of the motor was calculated as 92.3%. In addition, it is seen that the other calculated motor parameters are close to the values calculated because of the ANSYS-Maxwell.

CONFLICT OF INTEREST

The authors declare no conflict of interest.

REFERENCES

Bala, M. J., Roy, D. & Sengupta, A. (2020, 5-6 September). *The Performance Enhancement of BLDC Motor Using Halbach Array Rotor*. In: Proceedings of the 2020 IEEE 1st International Conference for Convergence in Engineering (ICCE), (pp. 405-409), Kolkata, India. https://www.doi.org/10.1109/ICCE50343.2020.9290642

Bapayya, N. K., & Venkata, R. K. (2020). Direct instantaneous torque control of Brushless DC motor using firefly Algorithm based fractional order PID controller. *Journal of King Saud University- Motorering Sciences*, *32*(2), 133-140. https://www.doi.org/10.1016/j.jksues.2018.04.007

Dusane, P. M. (2016). *Simulation of a Brushless DC Motor in ANSYS- Maxwell 3D, Prague*. MSc Thesis, Czech Technical University in Prague.

Ibrahim, H. E. A., Hassan, F. N., & Anas, O. (2014). Optimal PID control of a brushless DC motor using PSO and BF techniques. *Ain Shams Motorering Journal*, *5*(2), 391-398. https://www.doi.org/10.1016/j.asej.2013.09.013

Kannojia, P., & Chinmaya, K. A. (2023, 3-5 January). *Comparative Review and Finite Element Analysis of Energy Efficient Motors*. In: Proceedings of the International Conference on Power Electronics and Energy (ICPEE), Bhubaneswar, India. https://www.doi.org/10.1109/ICPEE54198.2023.10059611

Kumar, R., Kumar, P., Kumar, B., Singh, P., Kumar, R., & Kumar, A. (2022, 24-25 June). *Design and Analysis of High performance of a BLDC Motor for Electric Vehicle*. In: Proceedings of the 2nd International Conference on Emerging Frontiers in Electrical and Electronic Technologies (ICEFEET), Patna, India. https://www.doi.org/10.1109/ICEFEET51821.2022.984830

Kumar, A., Gandhi, R., Wilson, R. & Roy, R. (2020, 18-21 October). *The impact of different slot design of BLDC motor in a complete drive system*. In: Proceedings of the 46th Annual Conference of the IEEE Industrial Electronics Society, Singapore. https://www.doi.org/10.1109/IECON43393.2020.9255391

Özüpak, Y., & Aslan, E. (2023). Researching Inductive Power Transfer For Next Generation Electric Vehicles. *Ejons International Journal*, *7*(2), 220-232. https://www.doi.org/0.5281/zenodo.8265795